Exploration of the Potential Mechanisms of Lingqihuangban Granule for Treating Diabetic Retinopathy Based on Network Pharmacology

Shuai He
Shanghai General Hospital, Shanghai Jiaotong University School of Medicine https://orcid.org/0000-0002-3025-4226
Chufeng Gu
Shanghai General Hospital
Tong Su
Shanghai General Hospital
Chuandi Zhou
Shanghai General Hospital
Thashi Lhamo
Shanghai General Hospital
Deji Draga
Shanghai General Hospital
Lili Yin
Shanghai General Hospital
Qinghua Qiu (qinghuaqiu@163.com)
Shanghai Jiao Tong University School of Medicine https://orcid.org/0000-0002-8383-892X

Research

Keywords: Lingqihuangban Granule, diabetic retinopathy, network pharmacology, Chinese herbal compound

Posted Date: October 16th, 2020

DOI: https://doi.org/10.21203/rs.3.rs-90763/v1

Version of Record: A version of this preprint was published at Combinatorial Chemistry & High Throughput Screening on April 7th, 2022. See the published version at

https://doi.org/10.2174/1386207325666220407112018.

Abstract

Background: The Lingqihuangban Granule (LQHBG), a remarkable Chinese herbal compound, has been used for decades to treat diabetic retinopathy (DR) in Department of Ophthalmology, Shanghai General Hospital (National Clinical Research Center for Eye Diseases) with obvious effects. Through the method of network pharmacology, the present study constructed bioactive component-relative targets and protein-protein interaction network of the LQHBG and implemented gene function analysis and pathway enrichment of targets, discussing the mechanisms of traditional Chinese medicine LQHBG in treating DR.

Materials and methods: The bioactive ingredients of LQHBG were screened and obtained using TCMSP and ETCM databases, while the potential targets of bioactive ingredients were predicted by SwissTargetPrediction and ETCM databases. Compared with the disease target databases of TTD, Drugbank, OMIM and DisGeNET, the therapeutic targets of LQHBG for DR were extracted. Based on DAVID platform, GO annotation and KEGG pathway analyses of key targets were explored, combined with the screening of core pathways on Omicshare database and pathway annotation on Reactome database.

Results: A total of 357 bioactive components were screened from LQHBG, involving 86 possible targets of LQHBG treating DR. In PPI network, INS and ALB were identified as key genes. The effective targets were enriched in multiple signaling pathways, such as PI3K/Akt and MAPK pathways.

Conclusion: This study revealed the possible targets and pathways of LQHBG treating DR, reflecting the characteristics of multicomponent, multitarget and multipathway treatment of a Chinese herbal compound, and provided new ideas for further discussion.

Background

Diabetic retinopathy (DR) is a multifactorial neuromicrovascular complication of diabetes mellitus, serving as a main cause of blindness among working-aged people [1]. According to recent epidemiological studies, one-third of diabetic patients worldwide suffer from variant periods of DR, greatly increasing the economic and psychological burdens to individuals and society [2]. Currently, the treatment of DR is limited to laser photocoagulation of the retina and anti-vascular endothelial growth factor (VEGF) medications, accompanied by endocrine therapy and surgical methods, both of which have serious side effects and poor long-term prognosis, such as increased intraocular pressure, reverse aggravation of neovascularization and severe retinal hemorrhage [3, 4]. Therefore, it is urgent to seek potential targets and to explore new treatment methods and strategies.

Traditional Chinese Medicine (TCM) holds the opinion that diabetic retinopathy is associated with bad mood, tiredness and unhealthy diet [5], causing internal heat accumulation and damage to the liver, spleen, and kidney in the five internal organs. Then, deficiency of the Qi and imbalance of Yin and Yang bring about impaired blood circulation, such as congestion and hypoperfusion of the retinal microvasculature [6]; thus, the therapies of balancing Yin and Yang, promoting blood circulation and removing blood stasis are adopted in clinical practice. Traditional Chinese Medicine is a comprehensive

drug therapy that is widely used in Asian countries and that is gaining increasing amounts of attention and wide acceptance for its synergistic effect of multiple ingredients and minor side effects [7, 8]. Thus far, traditional Chinese medicine has shown its unique superiority and remarkable effects on the prevention and treatment of DR and has broad development prospects [9].

The LQHBG is a remarkable, prevalent Chinese herbal compound, consisting of Cistanche (Roucongrong), Lucid ganoderma (Lingzhi), Lycium barbarum (Gouqizi), Angelica sinensis (Danggui), Semen Cuscutae (Tusizi), Rhizoma atractylodis (Cangzhu), Ligusticum wallichii (Chuanxiong), Salvia miltiorrhiza (Danshen) and Codonopsis pilosula (Dangshen). It has been used for decades in Department of Ophthalmology, Shanghai General Hospital (National Clinical Research Center for Eye Diseases), with obvious effects, and many research articles have been published. According to the theory of traditional Chinese medicine, the spleen is the biochemical source of Qi and blood, with the prescription of Codonopsis pilosula possessing the functions of nourishing the spleen and stomach, benefiting Qi and blood, and Rhizoma atractylodis tonifying the spleen and reducing dampness. Cistanche, Semen Cuscutae and Lycium barbarum all benefit the kidney and essence, regulating the balance of Yin and Yang in the kidney. Among them, Lycium barbarum nourishes the liver and improves eyesight. In addition, Ligusticum wallichii and Salvia miltiorrhiza promote blood circulation and regulate Qi and blood transportation, while Lucid ganoderma serves as a treatment for fatigue syndrome and nourishes Qi and blood circulation. The LQHBG is a prescription mainly for tonifying the kidney and strengthening the spleen, treating DR and relieving the associated symptoms in many ways. Modern pharmacological studies show that some herbs of the LQHBG are capable of therapeutic effects on DR, such as Salvia miltiorrhiza [10, 11], Lycium barbarum [12, 13] and Rhizoma atractylodis, and the ingredients of single herbs also possess various functions [14, 15]. For example, by virtue of its remarkable antioxidant properties, Salvia miltiorrhiza elicits neuroprotective functions and prevents retinal neuronal apoptosis [16]. Its pharmacological effect of promoting blood circulation is applied to treat many blood circulation disorders, such as thrombosis, hypoperfusion, congestion and stasis [17]. It has been reported that Lycium barbarum prevents epithelial cell and neuronal apoptosis by regulating the Bcl-2/Bax and caspase3-mediated apoptotic pathway [18–20]. Kimura and Tsuneki's studies manifest that β-eudesmol isolated from Rhizoma atractylodis has a definite blocking effect in anti-angiogenic action through the inhibition of the ERK signaling pathway [14, 15]. However, the therapeutic effects of the remaining herbs on DR, such as Codonopsis pilosula, Semen Cuscutae and Cistanche, have not been reported in the literature, and the 9 herbs of the LQHBG have not been studied as a whole for their synergistic and complementary effects on DR. Moreover, the relationship between these potential targets and molecular pathways has not been studied; thus, the pharmacodynamic substance basis of the prescription and its pharmacological mechanism are not yet clear. Therefore, the systematic and overall study of the biological active components and molecular mechanisms of the LQHBG in the treatment of DR is conducive to providing new ideas for the innovation of clinical medication.

With the rapid development of modern biological information technology, network pharmacology comes into existence with the characteristics of multitarget, multicomponent and multipathway, providing effective screening and prediction of targets and potential mechanisms [21]. Based on the systems

biology theory, the network pharmacology approach establishes relational prediction models between drugs and related targets, diseases and therapeutic targets and integrates the interactive networks [22]. Through the analysis of components in various network modules and specific interactions between the nodes, the relationships between drugs and potential targets and the mechanisms therein are explored systemically and comprehensively [23, 24]. Using the network pharmacology as a method, this study explores the effective bioactive ingredients and relative targets of the LQHBG in the treatment of DR and reveals its molecular mechanism and interactions between herbs, which are of great significance for the clinical promotion of the LQHBG and the innovation of drug therapy.

Materials And Methods

1.1 Obtaining the single-herb chemical components of the LQHBG

The major chemical components of the single herb of LQHBG were searched on the Traditional Chinese Medicine Systems Pharmacology Database and Analysis Platform (TCSMP) [25] to construct a database of its pharmaceutical ingredients. According to the study results, the obtained bioactive components were screened by the absorption, distribution, metabolism and excretion parameters (ADME) with oral bioavailability (OB) ≥30% and drug-likeness (DL) ≥0.18.

Similarly, the chemical components of each herb were searched on another database called the Encyclopedia of Traditional Chinese Medicine (ETCM) [26] to acquire the corresponding supplementary bioactive compounds.

1.2 Prediction of targets of the chemical components and acquisition of disease-related targets

Based on the results produced by TCSMP database, the smile chemical structures of the compounds for each single herb were searched on the PubChem (https://pubchem.ncbi.nlm.nih.gov/) database [27], and then based on the structural characteristics of ligands, the predictive targets of the chemical components were gained by submitting them to the SwissTargetPrediction (http://www.swisstargetprediction.ch/) database [28]. The targets without detailed information were then filtered out. Regarding the bioactive compounds generated on ETCM database, the corresponding candidate target genes for each effective ingredient molecule were searched on the database. On the basis of the results, those with both a drug likeness grading higher than weak (i.e., such as moderate and good) and a prediction confidence index more than 0.80 were selected. Taking the above results from each database into consideration, the repetitive targets were filtered out, and the intersection was taken to construct a predictive targets database of the chemical components.

The index term DR was set to search on the Therapeutic Target Database (https://db.idrblab.org/ttd/) [29], the Drugbank database (https://www.drugbank.ca/) [30], the OMIM (https://omim.org/) [31] database and the DisGeNET database (http://www.disgenet.org/web/DisGeNET/menu/home) [32]. The results were summarized and the intersection was taken, and the known therapeutic targets of DR were then built.

1.3 Construction of the bioactive compound-targets network of LQHBG

Venn diagrams were utilized by importing gene names of the predictive targets of the chemical components and disease-related targets to analyze the same targets. With the filtered targets of the bioactive compounds of the LQHBG imported into Cytoscape (Version 3.6.0) [33], the bioactive compound-targets network was constructed. In the network, “node” represented the bioactive components of the LQHBG and relevant targets, while “edge” symbolized the interaction between bioactive compounds and targets. The relative network analysis of the characteristics of bioactive compounds and targets was employed to identify the significant nodes with the topology parameters of degree appearing dominant.

1.4 PPI network analysis and hub target screening

The target protein-protein interactions (PPIs) can be analyzed using the STRING (https://string-db.org/cgi/input.pl) online database [34]. The target information was imported into the STRING database with Homo sapiens being selected as the species and the comprehensive score of interactions by each pair of protein set at >0.4 as the screening condition to obtain the PPI information of the targets. Then, the PPI information was imported into Cytoscape software to visualize the PPI network of the interactive targets. The topological properties were analyzed through the Network analyzer function of the software with the two main network topology parameters of degree (degree) and close to the central (closeness centrality) on the key targets of the PPI network diagram. In addition, with regard to the target genes, the cytoHubba plug-in was adopted to calculate the top ten nodes ranked by Maximal Clique Centrality (MCC) scores that were the same as hub genes serving as supplementary. Meanwhile, the MCODE analysis tool in Cytoscape software was used to screen the modules in the PPI network diagram that may have significant interaction relationships. Moreover, the interactions among the crucial nodes were analyzed by consulting related literature.

1.5 GO biofunctional process and KEGG enrichment analysis of metabolic pathways

As Gene ontology (GO) biofunctional process and pathway analysis may reveal the degree of importance for variant gene targets and signal pathways among the protein-protein interaction network, this study made the use of DAVID (Version 6.8) platform [35] to conduct GO pathway analysis of the significant targets. Then, upon combining the Omicshare database screening core targets and pathways, the outcome was manifested in the form of a bubble diagram to illustrate the dynamic GO and KEGG analyses results. According to the enrichment factor value, the enrichment degree of core pathways was analyzed, aiming at exploring the probable mechanisms of the LQHBG in the treatment of DR. Furthermore, the annotation was added to the filtered core pathways using the Reactome database [36], and related graphics were created.

1.6 Molecular docking

We used the RCSB PDB platform (http://www.rcsb.org/pdb/home/home.do) [37] and downloaded the 3D structure documents of the key target proteins and used the PubChem database and downloaded the 3D structures of the bioactive compounds. The docking calculation was performed using the Yinfo Cloud Computing Platform for molecular docking verification, a friendly and versatile web server for biomedicinal, material, and statistical studies (https://cloud.yinfotek.com).

Results

2.1 Screening the components of the LQHBG

This study retrieved the reported nine herbs of the LQHBG and the screening conditions of the ADME parameters through the TCSMP database. Setting the indicators of OB≥30% and DL ≥0.18 to the active ingredients of each herb, we were able to obtain the results for 6 effective molecules for Cistanche, 61 for Lucid ganoderma, 45 for Lycium barbarum, 2 for Angelica sinensis, 11 for Semen Cuscutae, 9 for Rhizoma atractylodis, 7 for Ligusticum wallichii, 65 for Salvia miltiorrhiza and 21 for Codonopsis pilosula, for a total of 227 bioactive components. On the ETCM database, the drug likeness grading higher than weak and the prediction confidence index more than 0.80 were chosen. After removing the unrelated chemical components and complementing the bioactive compounds through searching the literature, chemical components with high content and clear pharmacological effects were also used as candidate active components, though they did not meet the ADME parameters. As a result, another 1 effective molecule for Cistanche, 46 for Lucid ganoderma, 8 for Lycium barbarum, 23 for Angelica sinensis, 2 for Semen Cuscutae, 5 for Rhizoma atractylodis, 15 for Ligusticum wallichii, 17 for Salvia miltiorrhiza and 13 for Codonopsis pilosula, for a total of 130 bioactive components, were added. Ultimately, a sum of 357 corresponding bioactive compounds was collected. The specific information of the partial herbs of Cistanche Angelica sinensis, Semen Cuscutae and Ligusticum wallichii through TCSMP is shown in table 1. The complete data set is provided in the attachment.

Table 1
Bioactive ingredient of partial herbs of the LQHBG

Mol ID	Molecule Name	*OB(%)*	*DL*	Single Herb
MOL000358	beta-sitosterol	36.91	0.75	Cistanche
MOL005320	arachidonate	45.57	0.2	Cistanche
MOL005384	suchilactone	57.52	0.56	Cistanche
MOL007563	Yangambin	57.53	0.81	Cistanche
MOL000098	quercetin	46.43	0.28	Cistanche
MOL008871	Marckine	37.05	0.69	Cistanche
MOL000358	beta-sitosterol	36.91	0.75	Angelica sinensis
MOL000449	Stigmasterol	43.83	0.76	Angelica sinensis
MOL001558	sesamin	56.55	0.83	Semen Cuscutae
MOL000184	NSC63551	39.25	0.76	Semen Cuscutae
MOL000354	isorhamnetin	49.6	0.31	Semen Cuscutae
MOL000358	beta-sitosterol	36.91	0.75	Semen Cuscutae
MOL000422	kaempferol	41.88	0.24	Semen Cuscutae
MOL005043	Campesterol	37.58	0.71	Semen Cuscutae
MOL005440	Isofucosterol	43.78	0.76	Semen Cuscutae
MOL005944	matrine	63.77	0.25	Semen Cuscutae
MOL006649	sophranol	55.42	0.28	Semen Cuscutae
MOL000953	CLR	37.87	0.68	Semen Cuscutae
MOL000098	quercetin	46.43	0.28	Semen Cuscutae
MOL001494	Mandenol	42	0.19	Ligusticum wallichii
MOL002135	Myricanone	40.6	0.51	Ligusticum wallichii
MOL002140	Perlolyrine	65.95	0.27	Ligusticum wallichii
MOL002151	senkyunone	47.66	0.24	Ligusticum wallichii
MOL002157	wallichilide	42.31	0.71	Ligusticum wallichii
MOL000359	sitosterol	36.91	0.75	Ligusticum wallichii
MOL000433	FA	68.96	0.71	Ligusticum wallichii

2.2 Selected targets

From 357 candidate compounds in the 9 herbs of LQHBG, a total of 3067 targets were predicted by the PubChem and SwissTargetPrediction databases, with 343, 532, 398, 140, 190, 150, 348, 550, and 416, respectively, for Cistanche, Lucid ganoderma, Lycium barbarum, Angelica sinensis, Semen Cuscutae, Rhizoma atractylodis, Ligusticum wallichii, Salvia miltiorrhiza, and Codonopsis pilosula, and a total of 1322 targets were acquired by the ETCM database, with 37, 320, 122, 47, 76, 238, 115, 134, and 233, respectively, for the above 9 herbs. Taking the intersection, we obtained 379 predictive targets without repetition for Cistanche, 763 for Lucid ganoderma, 489 for Lycium barbarum, 179 for Angelica sinensis, 233 for Semen Cuscutae, 353 for Rhizoma atractylodis, 436 for Ligusticum wallichii, 649 for Salvia miltiorrhiza and 593 for Codonopsis pilosula, for a total of 4073 targets. By searching the TTD, Drugbank, OMIM and Disgenet databases, the relevant targets of DR were obtained, with 8, 6, 59 and 246 targets being retrieved, respectively. After the repeated targets were deleted, 295 DR-related targets remained.

After drawing Venn diagrams of component-related targets and disease-related targets, 17 overlapping targets were obtained for Cistanche, 51 for Lucid ganoderma, 58 for Lycium barbarum, 39 for Angelica sinensis, 36 for Semen Cuscutae, 27 for Rhizoma atractylodis, 31 for Ligusticum wallichii, 46 for Salvia miltiorrhiza and 53 for Codonopsis pilosula, i.e., the targets related to the therapeutic effect of the active components of the LQHBG on DR. After the overlapping targets were deleted, 86 DR-related targets of the LQHBG action remained. The relevant information from the targets is shown in table 2, ranked randomly. The complete data set is provided in the attachment.

Table 2
Information of potential targets from active ingredients of the LQHBG

Num	*Gene*	Protein Name	Num	*Gene*	Protein Name
1	*VDR*	vitamin D receptor	22	*FAAH*	fatty acid amide hydrolase
2	*ALOX15*	arachidonate 15-lipoxygenase	23	*HIF1A*	hypoxia inducible factor 1 subunit alpha
3	*MMP2*	matrix metallopeptidase 2	24	*CNR1*	cannabinoid receptor 1
4	*PLG*	plasminogen	25	*MMP9*	matrix metallopeptidase 9
5	*KDR*	kinase insert domain receptor	26	*ACE*	angiotensin I converting enzyme
6	*GLO1*	glyoxalase I	27	*FLT1*	fms related tyrosine kinase 1
7	*PTPN1*	protein tyrosine phosphatase, non-receptor type 1	28	*SDHB*	succinate dehydrogenase complex iron sulfur subunit B
8	*NOS2*	nitric oxide synthase 2	29	*RBP4*	retinol binding protein 4
9	*MMP3*	matrix metallopeptidase 3	30	*NOS1*	nitric oxide synthase 1
10	*NOS3*	nitric oxide synthase 3	31	*ICAM1*	intercellular adhesion molecule 1
11	*AKR1B10*	aldo-keto reductase family 1 member B10	32	*PPARA*	peroxisome proliferator activated receptor alpha
12	*CYP2C19*	cytochrome P450 family 2 subfamily C member 19	33	*RAF1*	Raf-1 proto-oncogene, serine/threonine kinase
13	*KEAP1*	kelch like ECH associated protein 1	34	*AGTR1*	angiotensin II receptor type 1
14	*ALB*	albumin	35	*TGFB1*	transforming growth factor beta 1
15	*SERPINE1*	serpin family E member 1	36	*PTGS2*	prostaglandin-endoperoxide synthase 2
16	*CTSD*	cathepsin D	37	*FLT4*	fms related tyrosine kinase 4
17	*MME*	membrane metalloendopeptidase	38	*EP300*	E1A binding protein p300
18	*IGF1R*	insulin like growth factor 1 receptor	39	*C5AR1*	complement C5a receptor 1
19	*AKR1A1*	aldo-keto reductase family 1 member A1	40	*GLUL*	glutamate-ammonia ligase
20	*AKR1B1*	aldo-keto reductase family 1	41	*MAPK3*	mitogen-activated protein

		member B		kinase 3
21	*PPARG*	peroxisome proliferator activated receptor gamma	——	

2.3 Bioactive compound-target internet analysis of the LQHBG

To analyze the bioactive components screened from the LQHBG and the relevant targets for DR, Cytoscape software was used to construct the component-target network, as shown in figure 1. In the figure, the purple circle represented the active components, with 357 in total, the pink circle represented the relevant targets, with 86 in total, and the vermilion circle represented the 9 single herbs of LQHBG. There were 7 active components in Cistanche, which acted on 17 targets in the network diagram; Lucid ganoderma contained 107 active components, which acted on 51 targets; Lycium barbarum contained 53 active components, which acted on 58 targets; Angelica sinensis contained 24 active components, which acted on 39 targets; Semen Cuscutae contained 13 active components, which acted on 36 targets; Rhizoma atractylodis contained 14 active components, which acted on 27 targets; Ligusticum wallichii contained 22 active components, which acted on 31 targets; Salvia miltiorrhiza contained 82 active components, which acted on 46 targets; and Codonopsis pilosula contained 34 active components, which acted on 53 targets. In the network diagram, sitosterol (degree=36), quercetin (degree=34), Mandenol (degree=28) of Lycium barbarum and luteolin (degree=32) of Codonopsis pilosula had the highest degrees among the active ingredients in the LQHBG, followed by Lucidumol A (degree=22), Ganodermanondiol (degree=20) of Lucid ganoderma and NSC63551(degree=22) of Rhizoma atractylodis. However, the targets with high correlations with active components were CYP2C19 (degree=93), SERPINA6 (degree=89), PTPN1 (degree=83), VDR (degree=74), ALB (degree=71), and PPARA (degree=58). As seen from the active ingredient–target network diagram of the LQHBG, a single component can act on multiple targets at the same time, and correspondingly, a target can also be associated with multiple components at the same time, with the characteristics of multiple components and multiple targets.

2.4 PPI network analysis and hub target screening

The PPI network of the target is shown in figure 2 and contains 86 target proteins and 851 interaction edges, indicating close relationships between the targets. Among the red circles, the depth of the color represents the degree of the relationship between the edges, with the topological parameters of the degree algorithm being used, and the targets with degree > 50 were INS (degree = 63, closeness centrality = 0.812), ALB (degree = 60, closeness centrality = 0.788), GAPDH (degree = 58, closeness centrality = 0.774), TNF (degree = 54,Closeness centrality = 0.745), IL6 (degree = 52 closeness centrality = 0.726), and MAPK3 (degree = 51, closeness centrality = 0.726), suggesting that the six targets, INS, ALB, GAPDH, TNF, IL6 and MAPK3, are the core targets of the LQHBG treatment of DR in the PPI network and mediating

important roles in the network. The top ten hub genes containing the above 6 targets with the addition of MMP9, PTGS2, CASP3 and SERPINE1 were extracted by the use of the cytoHubba plug-in. In addition, through the MCODE analysis tool in Cytoscape software, two significant modules were selected from the PPI network diagram. The first module contained 31 target proteins and 381 protein interaction edges, with an MCODE score of 25.4, while the second module contained 8 target proteins and 13 interacting edges, with an MCODE score of 3.714.

2.5 Annotation analysis of gene functions and pathways

Annotation analysis of the gene functions and pathways of 84 important targets was carried out on the DAVID platform (Version 6.8), and the results were imported into the Omicshare database and Reactome database. To determine the screening and annotation of the core genes and pathways of the LQHBG components used for the treatment of DR, three diagrams (figures 3, 4 and table 3) were constructed with the use of GraphPad Prism 8.0 and R studio.

Table 3
Enrichment results of key targets (Top 20)

number	Pathway	count	Pvalue
ko04933	AGE-RAGE signaling pathway in diabetic complications	23	3.48E-24
ko04668	TNF signaling pathway	20	1.37E-18
ko04657	IL-17 signaling pathway	16	7.21E-15
ko04071	Sphingolipid signaling pathway	17	1.47E-14
ko04066	HIF-1 signaling pathway	15	8.08E-14
ko04660	T cell receptor signaling pathway	15	4.38E-13
ko04664	Fc epsilon RI signaling pathway	13	9.36E-13
ko04010	MAPK signaling pathway	21	1.27E-11
ko04064	NF-kappa B signaling pathway	14	3.31E-11
ko04150	mTOR signaling pathway	15	1.82E-10
ko04620	Toll-like receptor signaling pathway	13	2.73E-10
ko04920	Adipocytokine signaling pathway	11	1.12E-09
ko04622	RIG-I-like receptor signaling pathway	10	6.65E-09
ko04621	NOD-like receptor signaling pathway	14	8.73E-09
ko04350	TGF-beta signaling pathway	10	2.98E-08
ko04068	FoxO signaling pathway	11	1.62E-07
ko04370	VEGF signaling pathway	8	1.78E-07
ko04015	Rap1 signaling pathway	12	1.54E-06
ko04151	PI3K-Akt signaling pathway	15	5.58E-06

GO contains 3 subclasses, biological processes, cell components and molecular functions; 26 entries were enriched in biological processes, 10 entries were enriched in cell components and 16 entries were enriched in molecular functions, with the p-value being used as the significance standard of the enrichment degree. The top 10 items of the three subclasses of GO enriched by the targets are shown in figure 3. Among it, the red bar represented the biological processes, the green bar represented the cell components, and the blue bar represented the molecular functions.

There were 227 enriched KEGG pathways in total as the result of pathway analysis of the effective targets of the LQHBG. Figure 4 shows the effects of the related targets of the LQHBG mainly involved in many biological processes, such as cell cycle, the signal transduction, immune system, gene expression,

metabolism, and developmental biology, which reflected the LQHBG treatment of DR through regulating multiple complex biological processes, with the yellow to brown lines representing the importance of targets for enrichment of pathways and the p-value gradually increasing from yellow to brown. The bubble diagram of the top 20 pathways was significantly enriched by KEGG analysis and is shown in figure 5. After excluding extensive pathways, the top 20 signal transduction pathways are listed in table 4. After analysis, the 86 important targets were mainly distributed in the multiple pathways of advanced glycation end products (AGEs), phosphoinositol 3 kinase/protein kinase B (PI3K/Akt), mitogen-activated protein kinase (MAPK), transcriptional factor nuclear factor-κB (NF-κB), and transforming growth factor beta (TGF-β), indicating that the LQHBG treatment of DR acts on multiple pathways and that there is a complex interaction between these pathways.

Table 4
Docking score of ALB with bioactive components of LQHBG

Target Protein	PDB ID	Name	Grid Score	Grid vdw energy	Grid es energy	Internal energy repulsive	Cluster Size
ALB	1N5U	Ergosterol	-53.1529	-51.5407	-1.61218	12.05874	8
ALB	1N5U	5,6-Dihydroergosterol	-54.6588	-54.3065	-0.35225	27.25711	3
ALB	1N5U	Ganoderic Acid Am1	-65.4211	-50.3048	-15.1163	14.35782	8
ALB	1N5U	Ganoderic Acid B8	-67.3951	-57.6326	-9.76248	37.90099	8
ALB	1N5U	Ganoderic Acid C1	-56.4813	-46.0803	-10.401	33.76432	5
ALB	1N5U	Ganoderiol	-51.1042	-47.1751	-3.92914	17.13079	8
ALB	1N5U	Lucidenic	-54.9702	-46.4386	-8.53164	18.73997	8
ALB	1N5U	Lucidone	-47.5413	-43.3316	-4.2097	16.78487	4

2.6 Molecular docking

Based on the screening results of PPI, the molecular docking method was adopted in this study to verify the key target protein, ALB, as a representative. Its PDB ID was imported into the Yinfo Cloud Computing Platform, docking with the 8 corresponding bioactive components of the LQHBG. The docking results are shown in table 4. Among them, Grid Score resembles docking score, meaning that the smaller the value is, the stronger the binding force is. Grid vdw and Grid es contribute to van der Waals force (which can be understood as a nonpolar effect) and electrostatic force (which can be understood as a polar effect)

respectively. InternalEnergy refers to the repulsive force between the acceptor and ligand. After analyzing the docking results, it was noted that 2 were less than -60 kcal/mol, accounting for 25 percent, 5 were between -60 kcal/mol and -50 kcal/mol, taking up 62.5 percent, and 1 was higher than -40 kcal/mol, for 12.5 percent. In general, a grid score less than -40 kcal/mol indicates that the drug molecule and target have good binding activity, while a grid score greater than -40 kcal/mol indicates that the drug molecule has poor binding activity with the target. These findings indicate that the bioactive components of LQHBG have good binding activity with the key target. Moreover, Ganoderic Acid B8 of Lucid Ganoderma has the strongest bonding force according to the pattern diagram of interaction analysis shown in figure 6. Among it, the ball with stick represented the ligand, as with the bioactive components of LQHBG, while the slender rod represented the residues of the receptor, as with the key target protein ALB, with the dotted line standing for the interaction force.

Discussion

The Lingqihuangban Granule (LQHBG) is a classic prescription for treating diabetic retinopathy disease with blood stasis syndrome, consisting of 9 herbs of Cistanche, Lucid ganoderma, Lycium barbarum, Angelica sinensis, Semen Cuscutae, Rhizoma atractylodis, Ligusticum wallichii, Salvia miltiorrhiza and Codonopsis pilosula, altogether playing roles in treating DR. To determine the relationship between the bioactive ingredients of LQHBG and DR and the potential mechanism, this study constructed a biological network of interactions between bioactive components and relative targets. In this study, 357 bioactive components in the Lingqihuangban Granule were screened, acting on a total of 86 DR targets and involving 851 interaction relationships. As seen from the active components–targets network diagram, for single herbs, active ingredients such as sitosterol, quercetin, and fucosterol of Lycium barbarum can both regulate CYP2C19 and PPARA targets, while ALB, TNF, and MAPK3 can be influenced by more than one active ingredient, showing that the multiple targets can be mediated by multiple bioactive ingredients. Among the 9 diverse herbs, sitosterol is the common bioactive ingredient of Lycium barbarum, Lucid ganoderma, Angelica sinensis and Ligusticum wallichii with the same targets, and quercetin is the common bioactive ingredient of Lycium barbarum, Lucid ganoderma, Cistanche and Semen Cuscutae, indicating that there are synergistic effects between drugs. All of the above findings reflected the mechanisms of coordination and joint regulation of LQHBG in the treatment of DR and show that there were a variety of interactions among targets, which together constituted a complex biological network system.

In the PPI network diagram, the higher the degree of connectivity was, the greater the possibility of LQHBG treating DR through these targets was. The results showed that INS, ALB, GAPDH, TNF, IL6 and MAPK3 were the six core targets selected according to the degree ranking. Some of the effective genes have been identified by animal experiments and clinical tests. For example, INS is a gene that encodes insulin and plays a vital role in the regulation of carbohydrate and lipid metabolism and stimulates glucose uptake with the binding of the insulin receptor (INSR). Previous studies illustrated that INS^{C94Y} transgenic pigs developed a persistent diabetic phenotype, such as abnormalities of intraretinal

microvasculature similar to human beings, confirmed by regulating the functional proteins for Müller glial cell metabolism (e.g., GS) and the vital retinal water channel protein AQP4 [38]. Moore et al. reported that retinal microvascular endothelial cells (RMECs) treated with glycated albumin (AGE-Alb) gave rise to increases in the regulation of the NF-κB signaling pathway and leukocyte adhesion, accompanied by a dysfunctional blood–retinal barrier, while Treins et al. stated that AGE-Alb stimulated VEGF expression through an ERK-dependent pathway, playing an important role in the pathogenesis of proliferative diabetic retinopathy [39, 40]. Literature studies and network pharmacology results suggested that INS and ALB may be the key targets for the LQHBG treatment of DR, directly indicating the accuracy of network pharmacology in target prediction.

The results of DAVID (Version 6.8) Pathway and Reactome Pathway annotation analyses showed that the potential mechanisms of the LQHBG in the treatment of DR was mainly focused on the signaling pathways of biological metabolism, circulatory transport and anti-inflammatory and antioxidant functions. The diagram of the main effective pathways revealing the potential mechanisms of LQHBG for the treatment of DR is shown in Fig. 6. Based on the integration of pathway analysis and the theory of compatibility in traditional Chinese medicine, the Chinese herbal compound LQHBG played a hypoglycemic role of improving insulin resistance, reducing fat load and promoting the synthesis of liver glycogen. In addition, the components possess anti-inflammatory and antioxidant properties that regulate the synthesis of inflammatory factors and further prevent cell apoptosis and functional damage. At the same time, the herbs can effectively regulate blood circulation through reducing the oxidative stress response and preventing the proliferation of vascular endothelial cells, strengthening the adhesion of cells and the blood–retinal barrier (BRB). The above corresponded respectively with the theories of traditional Chinese medicine of invigorating spleen and benefiting digestion, tonifying kidney and warming Yang, nourishing blood and generating essence, with the result of clearing collaterals and clarifying eyes. To be specific, the pathways related to microvascular circulation include the AGE-RAGE pathway, the HIF-1α pathway and the VEGF pathway, which correspond to herbs containing the functions of strengthening Qi and blood and regulating the balance of Yin and Yang in the kidney, such as Lucid ganoderma, Salvia miltiorrhiza, Semen Cuscutae and Rhizoma atractylodis. All of the herbs acted on the AGE-RAGE signaling pathway, especially Lucid ganoderma and Salvia miltiorrhiza, reflecting the particularity and commonness of drug actions. The accumulation of AGEs plays a significant role in the progression of DR through exerting an inflammatory reaction and oxidative stress and increasing the expression of pro-apoptotic cytokines, which induce neurodegeneration, apoptosis of retinal pericytes and retinal microvascular dysfunction [41]. Brunelle et al. illustrated that AGEs activated the mitochondria-dependent apoptosis pathway by upregulating Bax expression and inhibiting Bcl-2 expression, participating in the release of pro-apoptotic cytochrome c from the mitochondria through the pores in the outer mitochondrial membrane, thus leading to the activation of caspase 9 and caspase 3 [42]. Moreover, the AGE-RAGE axis was linked to the blood-retinal barrier (BRB) breakdown through the mediation of leukocyte adherence barrier dysfunction, leading to the production of VEGF and angiogenic/vasopermeability growth factor in the retinal Müller glia [43] and to the activation of transcriptional factor nuclear factor-κB (NF-κB) and p38 MAPK expression, regulating pro-inflammatory

cytokine release [41, 44]. The quercetin of Lucid ganoderma, Lycium barbarum, and Semen Cuscutae and the luteolin of Salvia miltiorrhiza and Codonopsis pilosula mainly enriched the AGE-RAGE pathway and induced the apoptosis of retinal pericytes and neurons and mediated microvasculature dysfunction. Under hypoxia conditions, the production of hypoxia-inducible factor (HIF)-1α induces body glycolysis and erythrocytosis, giving rise to blood thickening and mitochondrial metabolism dysfunction [45]. Various clinical studies have confirmed that HIF-1α upregulates the transcription of the VEGF gene, stimulating angiogenesis and thus facilitating disease progression [46, 47]. The Ergosta-7,22-dien-3beta-yl palmitate in Lucid ganoderma, the sesamin in Semen Cuscutae and the epidanshenspiroketallactone in Salvia miltiorrhiza are mainly enriched in the HIF-1α pathway and prevent the occurrence of proliferative diabetic retinopathy (PDR) by reducing VEGF expression and suppressing angiogenesis.

The pathways related to biological metabolism include the sphingolipid signaling pathway and the PI3K-Akt signaling pathway, which corresponded to herbs containing the function of spleen's hypoglycemic effect through improving insulin resistance, reducing fat load and promoting the synthesis of liver glycogen, such as Codonopsis pilosula, Rhizoma atractylodis, Ligusticum wallichii and Lucid ganoderma. Evidence exists that the sphingolipid pathway is associated with inflammation and apoptosis through metabolic regulation [48]. A variety of sphingolipid metabolites, such as ceramide (Cer), ceramide-1-phosphate (C1P), sphingosine-1-phosphate (S1P), and lactosylceramide (LacCer), serve as the biologically active lipids, mediating important functions in biological metabolism and signal transduction [49]. Yaribeygi et al. illustrated that the upregulation of ceramides increases DR risk through inducing β-cell apoptosis and pancreatic inflammation [50], while Arai et al. reported that the accumulation of LacCer and S1P accelerate the proliferation of retinal endothelial cells and the eventual production of new blood vessels [51, 52]. The stigmasterone of Codonopsis pilosula, the NSC63551 of Rhizoma atractylodis, and the myricanone of Ligusticum wallichii mainly enrich the sphingolipid pathway and inhibit the synthesis and secretion of adipokines and proinflammatory cytokines. Recent studies have shown that the PI3K/Akt/VEGF signaling pathway gives rise to enhanced viability of retinal vascular endothelial cells (RVECs) and inhibition of angiogenesis and apoptosis, stimulated by miR-21 overexpression and phosphatase and tensin homolog (PTEN) suppression [53]. In addition, glycogen synthase kinase-3b (GSK3b) is a critical enzyme that reduces the synthesis of liver glycogen and increases the blood sugar concentration. Evidence has shown that the PI3K/Akt/GSK3 signaling pathway is involved in the metabolism of glycogen, playing a crucial role in the glucose output responsible for insulin resistance [54]. The stimulation of PI3K is essential for the insulin-stimulated glucose uptake, while phosphorylated Akt induces the prevention of GSK3 expression, which promotes glucose intake and inhibits the inflammatory response [55, 56]. The myricanone of Ligusticum wallichii and the lauric acid of Codonopsis pilosula mainly act on the PI3K/Akt pathway and regulate glucose metabolism and fat metabolism to resist the progression of insulin resistance. The pathways related to anti-inflammatory and antioxidant functions include the MAPK signaling pathway, the NF-kappa B signaling pathway and the NOD-like receptor signaling pathway, which correspond to herbs containing the functions of strengthening Qi and blood and regulating the balance of Yin and Yang in the kidney, such as Lycium barbarum, Angelica sinensis and Cistanche. The mitogen-activated protein kinase (MAPK) signaling

pathway is an important signal transduction pathway, consisting of p38 MAPK, JNK, and ERK and correlating to certain pathological processes, such as cell proliferation, apoptosis, inflammation, and necrosis [57]. Under the condition of injury, MAPK aggravates the inflammation in a vicious circle, with the downstream P-p38 MAPK entering the nucleus to release inflammatory factors, such as IL-1 and IL-18, and regulating the expression levels of Bax and Bcl-2 and the apoptosis effector protein Caspase-3, which is closely associated with apoptosis [58, 59]. The mandenol of Lycium barbarum and the quercetin of Cistanche may inhibit the MAPK signaling pathway and alleviate the inflammatory reaction and the progression of apoptosis. Nod-like receptor family pyrin domain-containing protein (NLRP) is closely related to the chronic inflammatory reaction and innate immune response, accompanied by high expression levels of proinflammatory molecules such as IL-1β and TNF-α in DR [60]. It has been reported that increased levels of NLRP3 inflammasomes exert downstream inflammatory cytokines and signal transduction of the NF-κB pathway, which induce a cascade of inflammatory response in the aggravation of DR [61]. The inosine of Lycium barbarum and the suchilactone of Roucourong mainly act on the NF-kappa B signaling pathway and the NOD-like receptor signaling pathway, which block the activation of the inflammatory response and the oxidation reaction in preventing abnormal biological processes.

In short, DR is characterized by structural and functional changes that are affected by multiple factors. The current clinical studies identified new targets for the treatment of DR and confirmed that the traditional Chinese medicine components acting on these potential targets play important roles in the prevention and treatment of DR. In this study, the bioactive components and targets of the LQHBG in treating DR were analyzed and predicted through a network pharmacology method, while the mechanisms of action of key genes and pathways were analyzed through bioinformatics methods. It can be seen from the network diagram of bioactive components–targets and pathway analysis that quercetin is most the common component of the four single drugs in the LQHBG, which act together on the core gene of ALB, reflecting the synergistic effects of compound Chinese medicine components. Each herb consists of different bioactive ingredients, acting on diverse drug targets, referred to as the AGE-RAGE, HIF-1a, PI3K Akt, MAPK, and NF-kappa B signaling pathways, treating DR from different therapeutic aspects of the circulation, metabolism, inflammation, and aging, embodying the complementary effects of compound Chinese medicine in the treatment of DR with multiple components, multiple targets and multiple approaches, providing a new idea for the treatment of DR with complex pathogenesis. Because the results of this study were only obtained from available databases and the obtained pathways were relatively wide, failing to fully elucidate the molecular regulation and interaction relationships, the next step will be undertaking in vitro experiments and performing analysis of the biological technology, further verifying the accuracy of the targets of the Chinese herbal compound LQHBG and will be focusing on each single pathway to study the molecular regulation and interaction relationships, further exploring the specific mechanisms of action of this Chinese herbal compound in treating DR.

Conclusion

This study obtained the bioactive ingredients of the LQHBG and the predictive targets of DR and then used network pharmacology to manifest the correlations between the Chinese herbal compound LQHBG

and DR and the potential synergistic mechanisms of the LQHBG for the treatment of DR, providing new ideas for drug treatment.

Abbreviations

Lingqihuangban Granule LQHBG

diabetic retinopathy DR

Traditional Chinese Medicine TCM

Traditional Chinese Medicine Systems Pharmacology Database and Analysis Platform TCMSP

oral bioavailability OB

drug-likeness DL

Encyclopedia of Traditional Chinese Medicine ETCM

Therapeutic Target Database TTD

Online Mendelian Inheritance in Man OMIM

protein-protein interaction PPI

Maximal Clique Centrality MCC

Database for Annotation, Visualization and Integrated Discovery DAVID

Gene Ontology GO

Kyoto Encyclopedia of Genes and Genomes KEGG

Albumin ALB

Insulin INS

insulin receptor INSR

advanced glycation end products AGEs

phosphatidylinositol-3-kinase PI3K

mitogen-activated protein kinase MAPK

transcriptional factor nuclear factor-κB NF-κB

transforming growth factor beta TGF – β

Retinal microvascular endothelial cells RMECs

glycated albumin AGE-Alb

blood–retinal barrier BRB

hypoxia-inducible factor HIF

proliferative diabetic retinopathy PDR

ceramide Cer

ceramide-1-phosphate C1P

sphingosine-1-phosphate S1P

and lactosylceramide LacCer

retinal vascular endothelial cells RVECs

phosphatase and tensin homolog PTEN

glycogen synthase kinase-3b GSK3b

Nod-like receptor family pyrin domain-containing protein NLRP

vascular endothelial growth factor VEGF

Declarations

Ethics approval and consent to participate

Not applicable.

Consent for publication

The manuscript is approved by all authors for publication.

Available of data and materials

All data generated or analyzed in this study are included in this article and its supplementary files.

Competing interests

The authors declare that they have no competing interests.

Funding

This work was supported by the National Natural Science Foundation of China (81970811), the National Science and Technology Major Project of China (2017ZX09304010), the National Key R&D Program of China (2016YFC0904800, 2019YFC0840607) and the Tibet Natural Science Foundation of China (XZ2017ZR-ZYZ09, XZ2018ZRG-95, XZ2018ZRG-100(Z)).

Authors' Contribution

All authors contributed significantly to this work. SH, CG and TS were participated in all aspects of this research involving data analysis, experimental performance and paper writing. CZ, TL and DD retrieved the literature and analyzed the data. QQ and LY contributed to the research design, supervision of the research, data analyses and revised the manuscript. All authors read and approved the final manuscript.

Acknowledgements

Not applicable.

References

1. Piao, C.L., et al., Utilizing network pharmacology to explore the underlying mechanism of Radix Salviae in DR. Chin Med, 2019. 14: p. 58.
2. Lee, R., T.Y. Wong, and C. Sabanayagam, Epidemiology of DR, diabetic macular edema and related vision loss. Eye Vis (Lond), 2015. 2: p. 17.
3. Zhao, Y. and R.P. Singh, The role of anti-vascular endothelial growth factor (anti-VEGF) in the management of proliferative DR. Drugs Context, 2018. 7: p. 212532.
4. Whitcup, S.M., et al., Pharmacology of Corticosteroids for Diabetic Macular Edema. Invest Ophthalmol Vis Sci, 2018. 59(1): p. 1-12.
5. Pang, B., et al., Traditional chinese medicine for diabetic retinopathy: A systematic review and meta-analysis. Medicine (Baltimore), 2020. 99(7): p. e19102.
6. Song, W. and Y.W. Zhu, Chinese Medicines in DR Therapies. Chin J Integr Med, 2019. 25(4): p. 316-320.
7. Li, S. and S. Xutian, New Development in Traditional Chinese Medicine: Symbolism-Digit Therapy as a Special Naturopathic Treatment. Am J Chin Med, 2016. 44(7): p. 1311-1323.

8. Li, S., B. Zhang, and N. Zhang, Network target for screening synergistic drug combinations with application to traditional Chinese medicine. BMC Syst Biol, 2011. 5 Suppl 1(Suppl 1): p. S10.
9. Xu, Z.H., et al., Progress in Experimental and Clinical Research of the DR Treatment Using Traditional Chinese Medicine. Am J Chin Med, 2018: p. 1-27.
10. Zhang, L., et al., Effect of Salvia miltiorrhiza on retinopathy. Asian Pac J Trop Med, 2013. 6(2): p. 145-9.
11. Manthey, A.L., K. Chiu, and K.F. So, Effects of Lycium barbarum on the Visual System. Int Rev Neurobiol, 2017. 135: p. 1-27.
12. Song, M.K., et al., Lycium barbarum (Goji Berry) extracts and its taurine component inhibit PPAR-γ-dependent gene transcription in human retinal pigment epithelial cells: Possible implications for DR treatment. Biochem Pharmacol, 2011. 82(9): p. 1209-18.
13. Yao, Q., et al., Lycium Barbarum Polysaccharides Improve Retinopathy in Diabetic Sprague-Dawley Rats. Evid Based Complement Alternat Med, 2018. 2018: p. 7943212.
14. Tsuneki, H., et al., Antiangiogenic activity of beta-eudesmol in vitro and in vivo. Eur J Pharmacol, 2005. 512(2-3): p. 105-15.
15. Kimura, I., Medical benefits of using natural compounds and their derivatives having multiple pharmacological actions. Yakugaku Zasshi, 2006. 126(3): p. 133-43.
16. Lin, T.H. and C.L. Hsieh, Pharmacological effects of Salvia miltiorrhiza (Salvia miltiorrhiza) on cerebral infarction. Chin Med, 2010. 5: p. 22.
17. Ng, C.S., et al., [Systematic review and meta-analysis of randomized controlled trials comparing Chinese patent medicines Compound Salvia miltiorrhiza Dripping Pills and Di'ao Xinxuekang in treating angina pectoris]. Zhong Xi Yi Jie He Xue Bao, 2012. 10(1): p. 25-34.
18. Hu, C.K., et al., The protective effects of Lycium barbarum and Chrysanthemum morifolum on diabetic retinopathies in rats. Vet Ophthalmol, 2012. 15 Suppl 2: p. 65-71.
19. Liu, L., et al., Lycium barbarum polysaccharides protected human retinal pigment epithelial cells against oxidative stress-induced apoptosis. Int J Ophthalmol, 2015. 8(1): p. 11-6.
20. Song, M.K., B.D. Roufogalis, and T.H. Huang, Reversal of the Caspase-Dependent Apoptotic Cytotoxicity Pathway by Taurine from Lycium barbarum (Goji Berry) in Human Retinal Pigment Epithelial Cells: Potential Benefit in DR. Evid Based Complement Alternat Med, 2012. 2012: p. 323784.
21. Zhang, R., et al., Network Pharmacology Databases for Traditional Chinese Medicine: Review and Assessment. Front Pharmacol, 2019. 10: p. 123.
22. Hopkins, A.L., Network pharmacology: the next paradigm in drug discovery. Nat Chem Biol, 2008. 4(11): p. 682-90.
23. Piao, C., et al., Network Pharmacology-based Investigation of the Underlying Mechanism of Panax notoginseng Treatment of DR. Comb Chem High Throughput Screen, 2020. 23(4): p. 334-344.
24. Boezio, B., et al., Network-based Approaches in Pharmacology. Mol Inform, 2017. 36(10).

25. Jinlong Ru; Peng Li; Jinan Wang; Wei Zhou; Bohui Li; Chao Huang; Pidong Li; Zihu Guo; Weiyang Tao; Yinfeng Yang; Xue Xu; Yan Li; Yonghua Wang; Ling Yang. TCMSP: a database of systems pharmacology for drug discovery from herbal medicines. J Cheminformatics. 2014 Apr 16;6(1):13.
26. Xu HY, Zhang YQ, Liu ZM, Chen T, Lv CY, Tang SH, Zhang XB, Zhang W, Li ZY, Zhou RR, Yang HJ, Wang XJ, Huang LQ. ETCM: an encyclopaedia of traditional Chinese medicine. Nucleic Acids Res. 2018 Oct 26.
27. Kim, S., Chen, J., Cheng, T., Gindulyte, A., He, J., He, S., Li, Q., Shoemaker, B. A., Thiessen, P. A., Yu, B., Zaslavsky, L., Zhang, J., & Bolton, E. E. (2019). PubChem 2019 update: improved access to chemical data. Nucleic acids research, 47(D1), D1102–D1109.
28. David Gfeller, Olivier Michielin, Vincent Zoete, Shaping the interaction landscape of bioactive molecules, Bioinformatics, Volume 29, Issue 23, 1 December 2013, Pages 3073–3079.
29. Y. X. Wang, S. Zhang, F. C. Li, Y. Zhou, Y. Zhang, R. Y. Zhang, J. Zhu, Y. X. Ren, Y. Tan, C. Qin, Y. H. Li, X. X. Li, Y. Z. Chen* and F. Zhu*. Therapeutic Target Database 2020: enriched resource for facilitating research and early development of targeted therapeutics. Nucleic Acids Research. 48(D1): D1031-D1041 (2020).
30. Wishart DS, Feunang YD, Guo AC, Lo EJ, Marcu A, Grant JR, Sajed T, Johnson D, Li C, Sayeeda Z, Assempour N, Iynkkaran I, Liu Y, Maciejewski A, Gale N, Wilson A, Chin L, Cummings R, Le D, Pon A, Knox C, Wilson M. DrugBank 5.0: a major update to the DrugBank database for 2018. Nucleic Acids Res. 2017 Nov 8. doi: 10.1093/nar/gkx1037.
31. Amberger JS, Bocchini CA, Schiettecatte F, Scott AF, Hamosh A. OMIM.org: Online Mendelian Inheritance in Man (OMIM®), an online catalog of human genes and genetic disorders. Nucleic Acids Res. 2015;43(Database issue):D789-D798.
32. Piñero J, Bravo À, Queralt-Rosinach N, et al. DisGeNET: a comprehensive platform integrating information on human disease-associated genes and variants. Nucleic Acids Res. 2017;45(D1):D833-D839.
33. Otasek, et al., Cytoscape Automation: empowering workflow-based network analysis Genome Biology, 20:185 (2019).
34. Szklarczyk D, Gable AL, Lyon D, et al. STRING v11: protein-protein association networks with increased coverage, supporting functional discovery in genome-wide experimental datasets. Nucleic Acids Res. 2019;47(D1):D607-D613.
35. Huang DW, Sherman BT, Lempicki RA. Systematic and integrative analysis of large gene lists using DAVID Bioinformatics Resources. Nature Protoc. 2009;4(1):44-57.
36. Kleinwort, K.J.H., et al., Retinopathy with central oedema in an INS (C94Y) transgenic pig model of long-term diabetes. Diabetologia, 2017. 60(8): p. 1541-1549.
37. H.M. Berman, J. Westbrook, Z. Feng, G. Gilliland, T.N. Bhat, H. Weissig, I.N. Shindyalov, P.E. Bourne. (2000) The Protein Data Bank Nucleic Acids Research, 28: 235-242.
38. assal B, Matthews L, Viteri G, Gong C, Lorente P, Fabregat A, Sidiropoulos K, Cook J, Gillespie M, Haw R, Loney F, May B, Milacic M, Rothfels K, Sevilla C, Shamovsky V, Shorser S, Varusai T, Weiser J, Wu

G, Stein L, Hermjakob H, D'Eustachio P. The reactome pathway knowledgebase. Nucleic Acids Res. 2020 Jan 8;48(D1):D498-D503. doi: 10.1093/nar/gkz1031.

39. Treins, C., et al., Regulation of vascular endothelial growth factor expression by advanced glycation end products. J Biol Chem, 2001. 276(47): p. 43836-41.
40. Moore, T.C., et al., The role of advanced glycation end products in retinal microvascular leukostasis. Invest Ophthalmol Vis Sci, 2003. 44(10): p. 4457-64.
41. XL, W., et al., AGEs Promote Oxidative Stress and Induce Apoptosis in Retinal Pigmented Epithelium Cells RAGE-dependently. Journal of molecular neuroscience : MN, 2015. 56(2): p. 449-60.
42. Czabotar, P.E., et al., Control of apoptosis by the BCL-2 protein family: implications for physiology and therapy. Nat Rev Mol Cell Biol, 2014. 15(1): p. 49-63.
43. H, Z., W. M, and S. AW, AGEs, RAGE, and DR. Current diabetes reports, 2011. 11(4): p. 244-52.
44. Zong, H., et al., Hyperglycaemia-induced pro-inflammatory responses by retinal Muller glia are regulated by the receptor for advanced glycation end-products (RAGE). Diabetologia, 2010. 53(12): p. 2656-66.
45. Goda, N. and M. Kanai, Hypoxia-inducible factors and their roles in energy metabolism. Int J Hematol, 2012. 95(5): p. 457-63.
46. Fu, Z., et al., Hypoxia-inducible factor-1α protects cervical carcinoma cells from apoptosis induced by radiation via modulation of vascular endothelial growth factor and p53 under hypoxia. Med Sci Monit, 2015. 21: p. 318-25.
47. Zhang, D., F.L. Lv, and G.H. Wang, Effects of HIF-1α on DR angiogenesis and VEGF expression. Eur Rev Med Pharmacol Sci, 2018. 22(16): p. 5071-5076.
48. M, M., et al., Contributions of amino acid, acylcarnitine and sphingolipid profiles to type 2 diabetes risk among South-Asian Surinamese and Dutch adults. BMJ open diabetes research & care, 2020. 8(1).
49. Mondal, K. and N. Mandal, Role of Bioactive Sphingolipids in Inflammation and Eye Diseases. Adv Exp Med Biol, 2019. 1161: p. 149-167.
50. Yaribeygi, H., et al., Ceramides and diabetes mellitus: an update on the potential molecular relationships. Diabet Med, 2020. 37(1): p. 11-19.
51. Arai, T., et al., Lactosylceramide stimulates human neutrophils to upregulate Mac-1, adhere to endothelium, and generate reactive oxygen metabolites in vitro. Circ Res, 1998. 82(5): p. 540-7.
52. Baeyens, A., et al., Exit Strategies: S1P Signaling and T Cell Migration. Trends Immunol, 2015. 36(12): p. 778-787.
53. Lu, J.M., et al., Repression of microRNA-21 inhibits retinal vascular endothelial cell growth and angiogenesis via PTEN dependent-PI3K/Akt/VEGF signaling pathway in DR. Exp Eye Res, 2020. 190: p. 107886.
54. G, Z., et al., viaSkimmin Improves Insulin Resistance Regulating the Metabolism of Glucose: and Models. Frontiers in pharmacology, 2020. 11: p. 540.

55. Yang, M., et al., Krüppel-like factor 14 increases insulin sensitivity through activation of PI3K/Akt signal pathway. Cell Signal, 2015. 27(11): p. 2201-8.
56. Ren, Z., et al., C-Phycocyanin inhibits hepatic gluconeogenesis and increases glycogen synthesis via activating Akt and AMPK in insulin resistance hepatocytes. Food Funct, 2018. 9(5): p. 2829-2839.
57. Akrami, H., et al., PlGF knockdown inhibited tumor survival and migration in gastric cancer cell via PI3K/Akt and p38MAPK pathways. Cell Biochem Funct, 2016. 34(3): p. 173-80.
58. Nadeem, A., et al., IL-17A causes depression-like symptoms via NFκB and p38MAPK signaling pathways in mice: Implications for psoriasis associated depression. Cytokine, 2017. 97: p. 14-24.
59. Feng, D., W.H. Ling, and R.D. Duan, Lycopene suppresses LPS-induced NO and IL-6 production by inhibiting the activation of ERK, p38MAPK, and NF-kappaB in macrophages. Inflamm Res, 2010. 59(2): p. 115-21.
60. 60.Yin, Y., et al., Resolvin D1 inhibits inflammatory response in STZ-induced DR rats: Possible involvement of NLRP3 inflammasome and NF-κB signaling pathway. Mol Vis, 2017. 23: p. 242-250.
61. Lim, R.R., et al., NOD-like Receptors in the Eye: Uncovering Its Role in DR. Int J Mol Sci, 2020. 21(3).

Figures

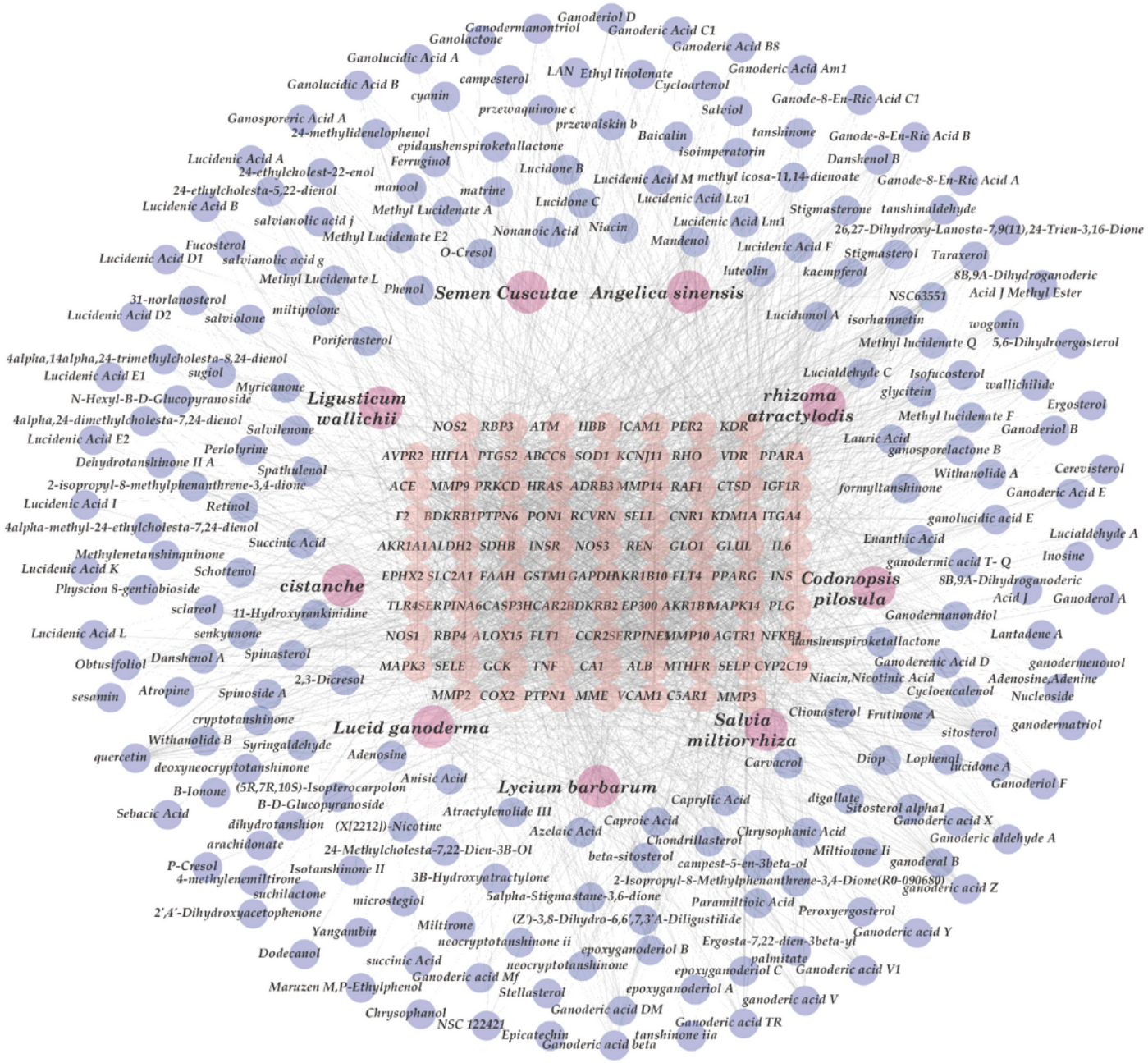

Figure 1

Ingredients-related targets network of the Lingqihuangban Granule. The purple circle represented the active components, the pink circle represented the relevant targets, and the vermilion circle represented the 9 single herbs of LQHBG.

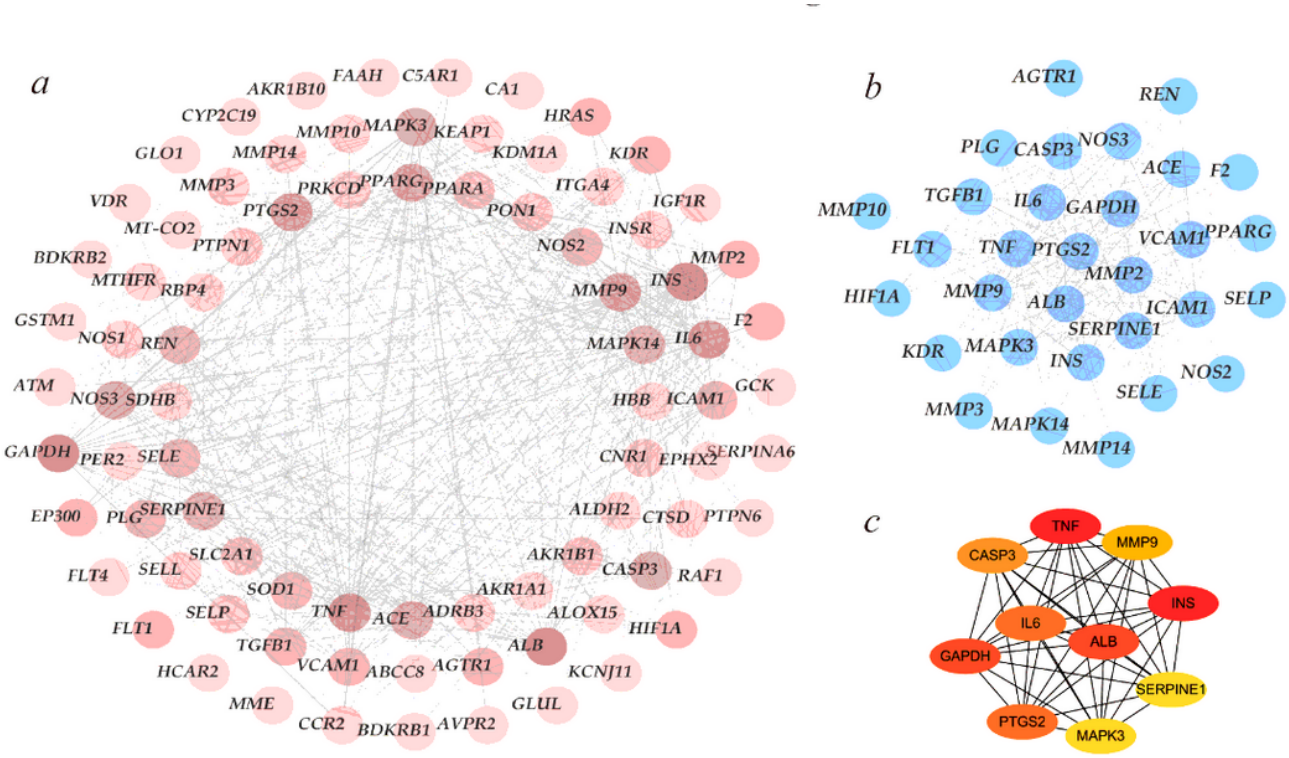

Figure 2

Protein-protein interaction network of the Lingqihuangban Granule a. Network diagram of PPI targets of the Lingqihuangban Granule. The depth of the color represented the degree of the relation between the edges b. Screening of significance modules in PPI network diagram. c. Screening of top 10 hub genes in PPI network diagram.

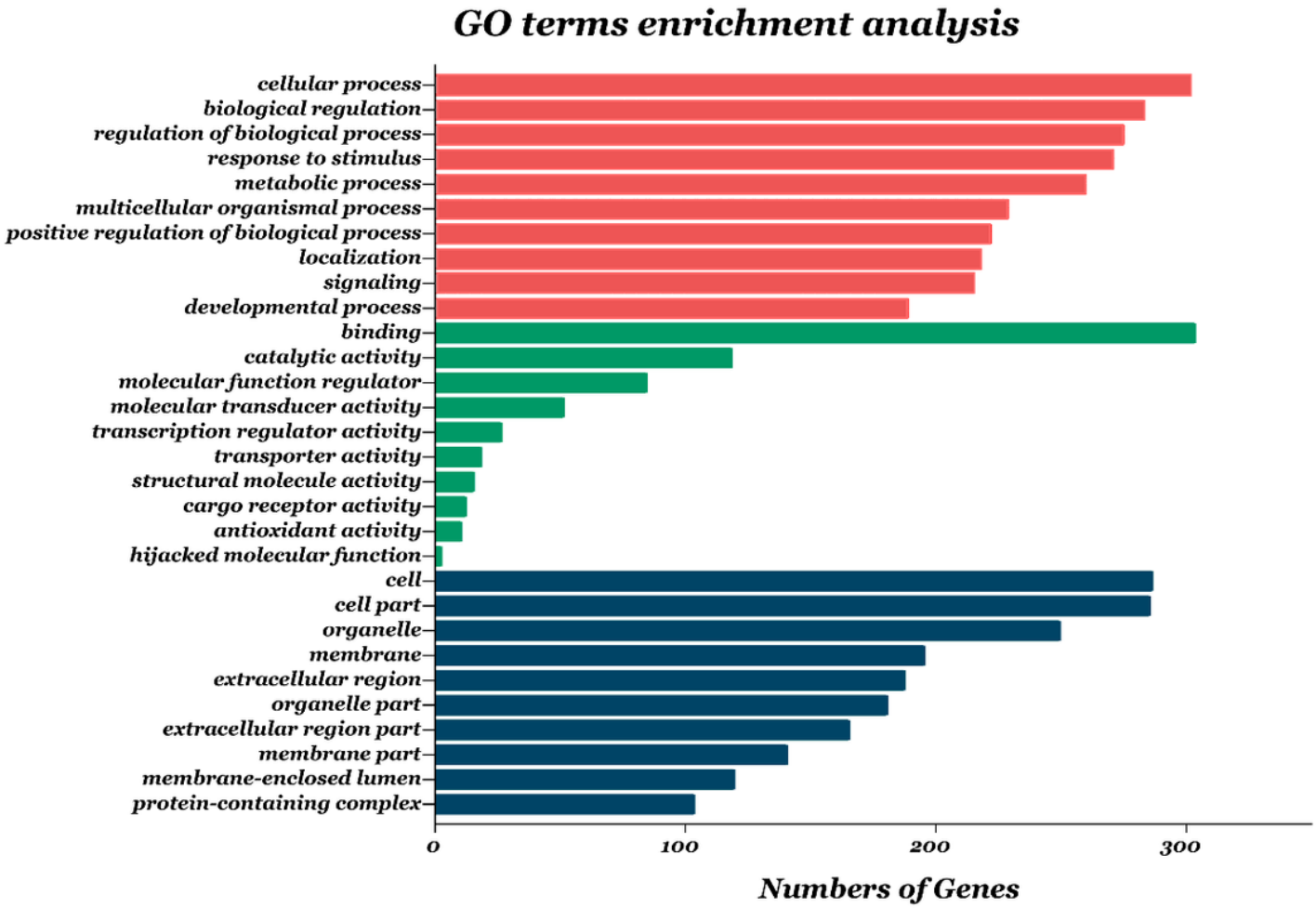

Figure 3

Functional annotation analysis of the targets. The red bar represented the biological processes, the green bar represented the cell components, and the blue bar represented the molecular functions.

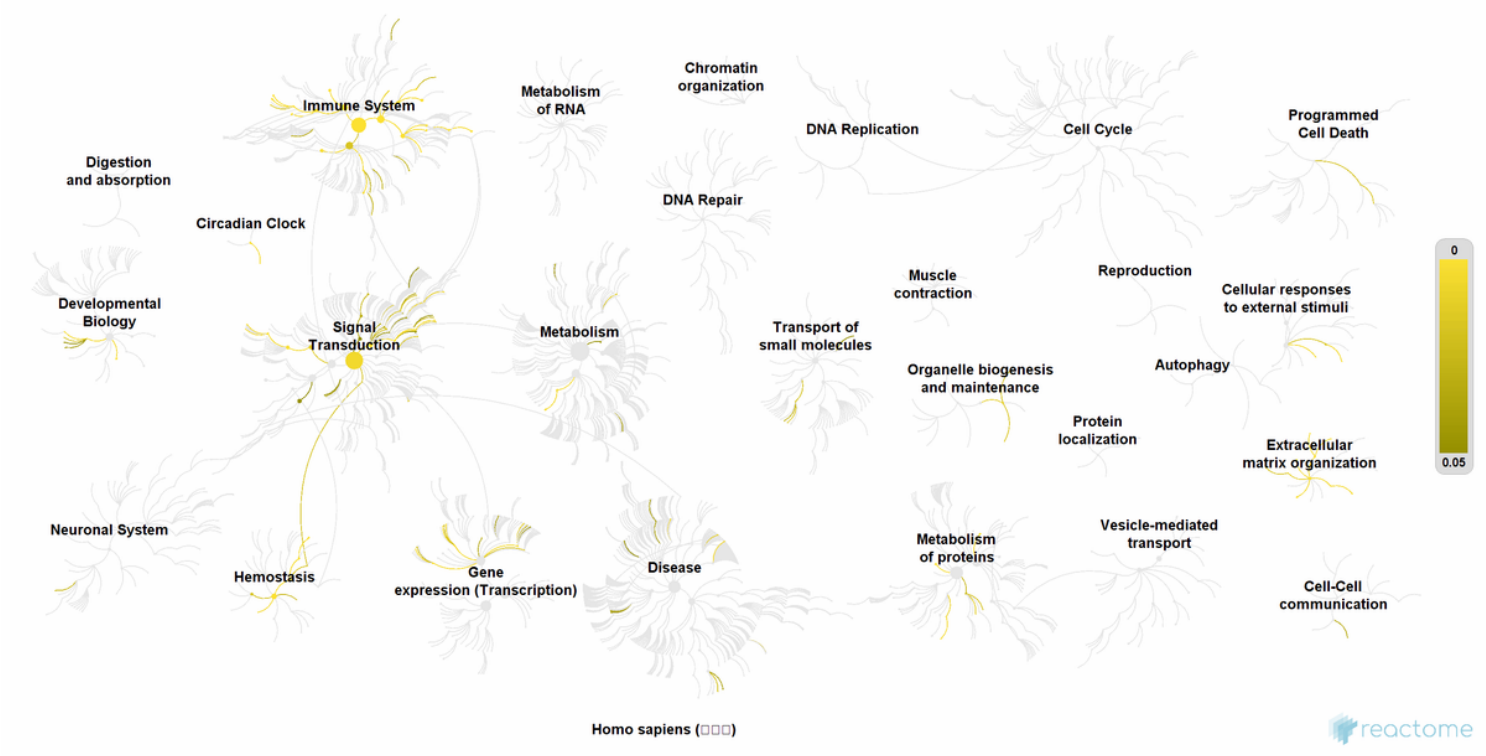

Figure 4

Biological function analysis of key targets for active ingredients of the LQHBG for treatment of DR performed on Reactome platform. The effect of relative targets of the LQHBG mainly involved in many biological processes such as cell cycle, the signal transduction, immune system, gene expression, metabolism, developmental biology and so on, with the yellow to brown lines representing the importance of targets for enrichment of pathways and the P value being gradually increasing from yellow to brown.

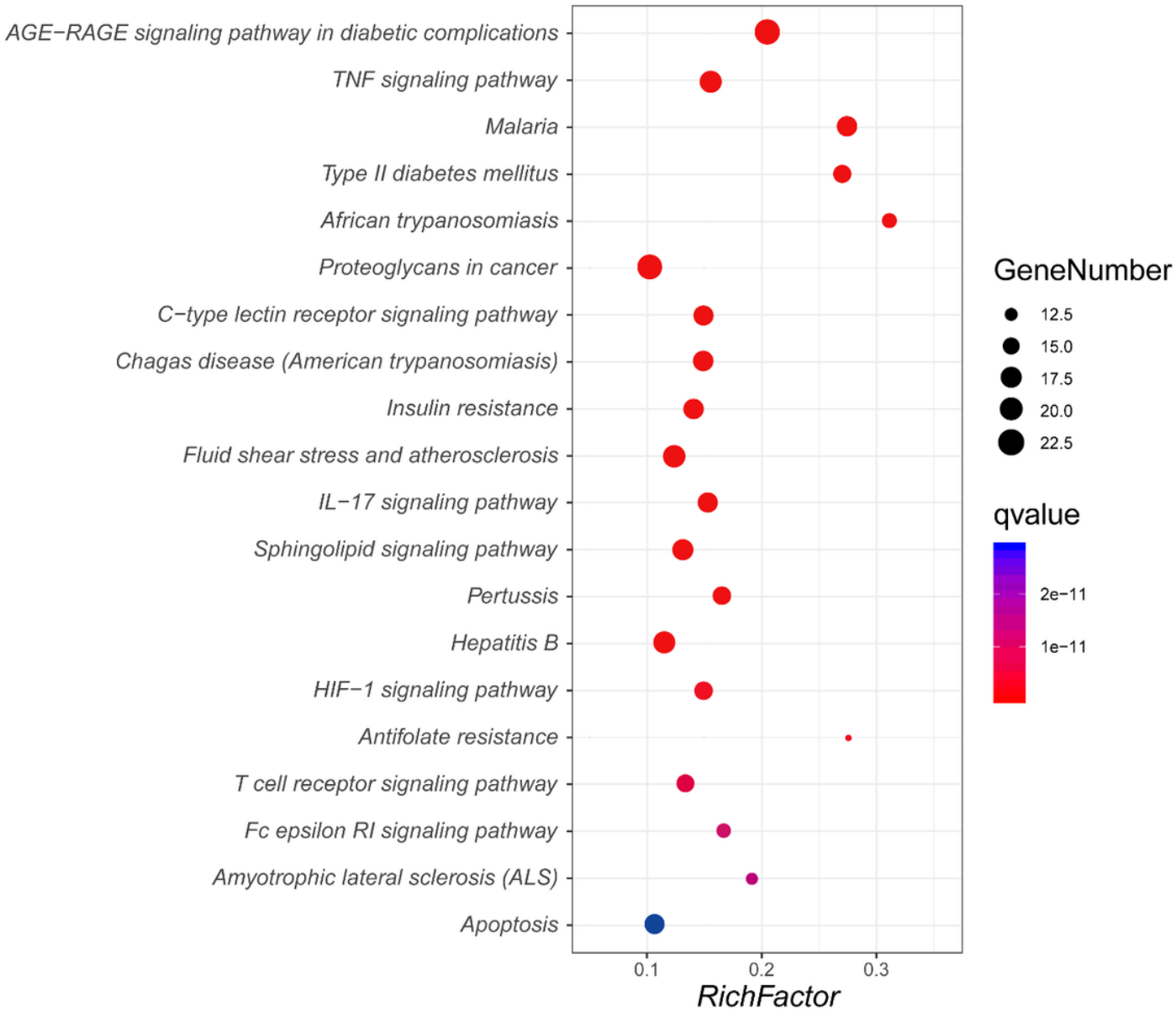

Figure 5

Bubble diagram of KEGG enrichment of top 20 key targets for the LQHBG for treatment of DR.

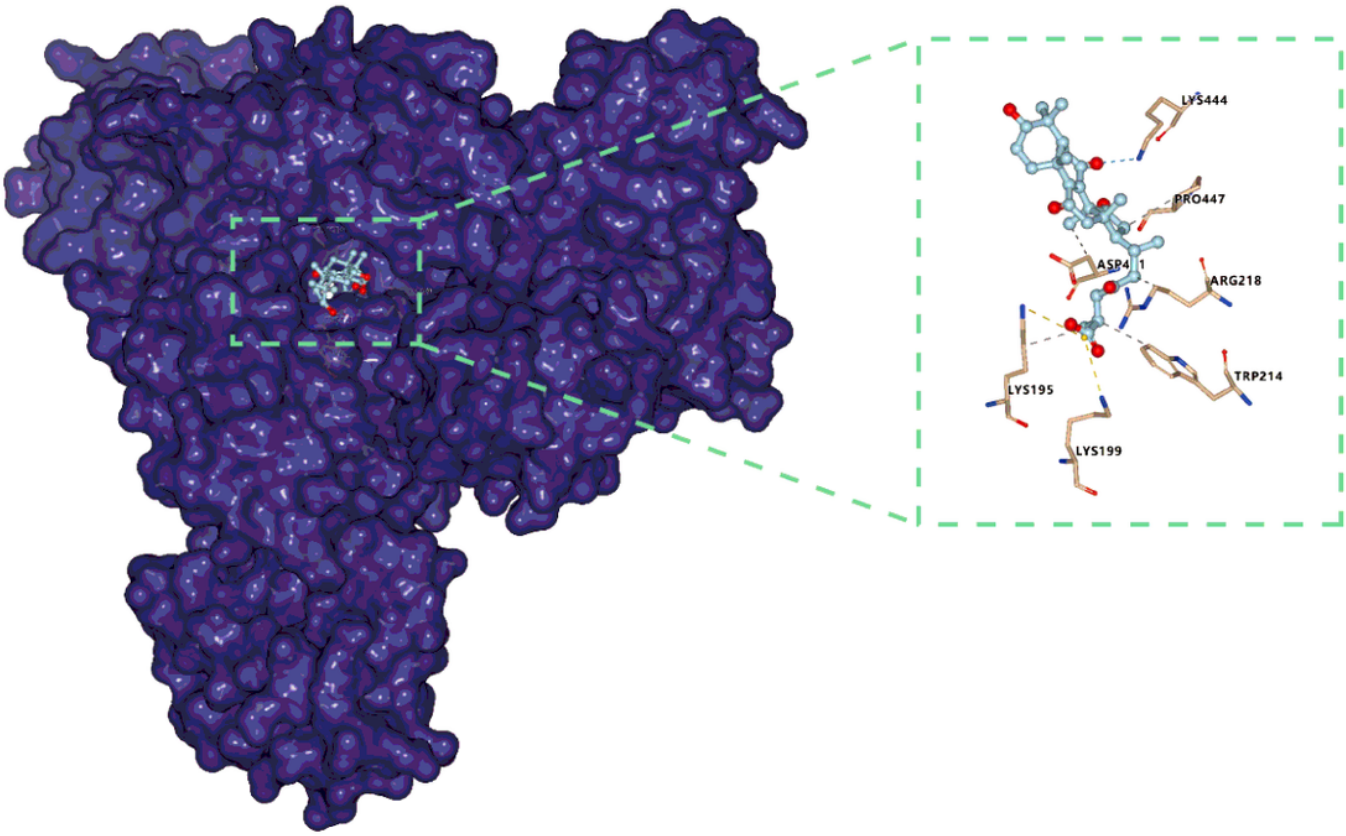

Figure 6

Molecular docking interaction model of Ganoderic Acid B8 of Lucid Ganoderma. The left part described the receptor of target protein ALB docking with the ligand of bioactive component of LQHBG, with the purple foam representing the surface of the receptor protein and the framed area showing the docking point. The right framed part manifested the the enlarged docking point. The ball with stick represented the ligand the same as bioactive components of LQHBG, the slender rod represented the residues of receptor the same as the key target protein ALB, the dotted line represented the interaction force and the name showed the serial number of the residues of receptor ALB.

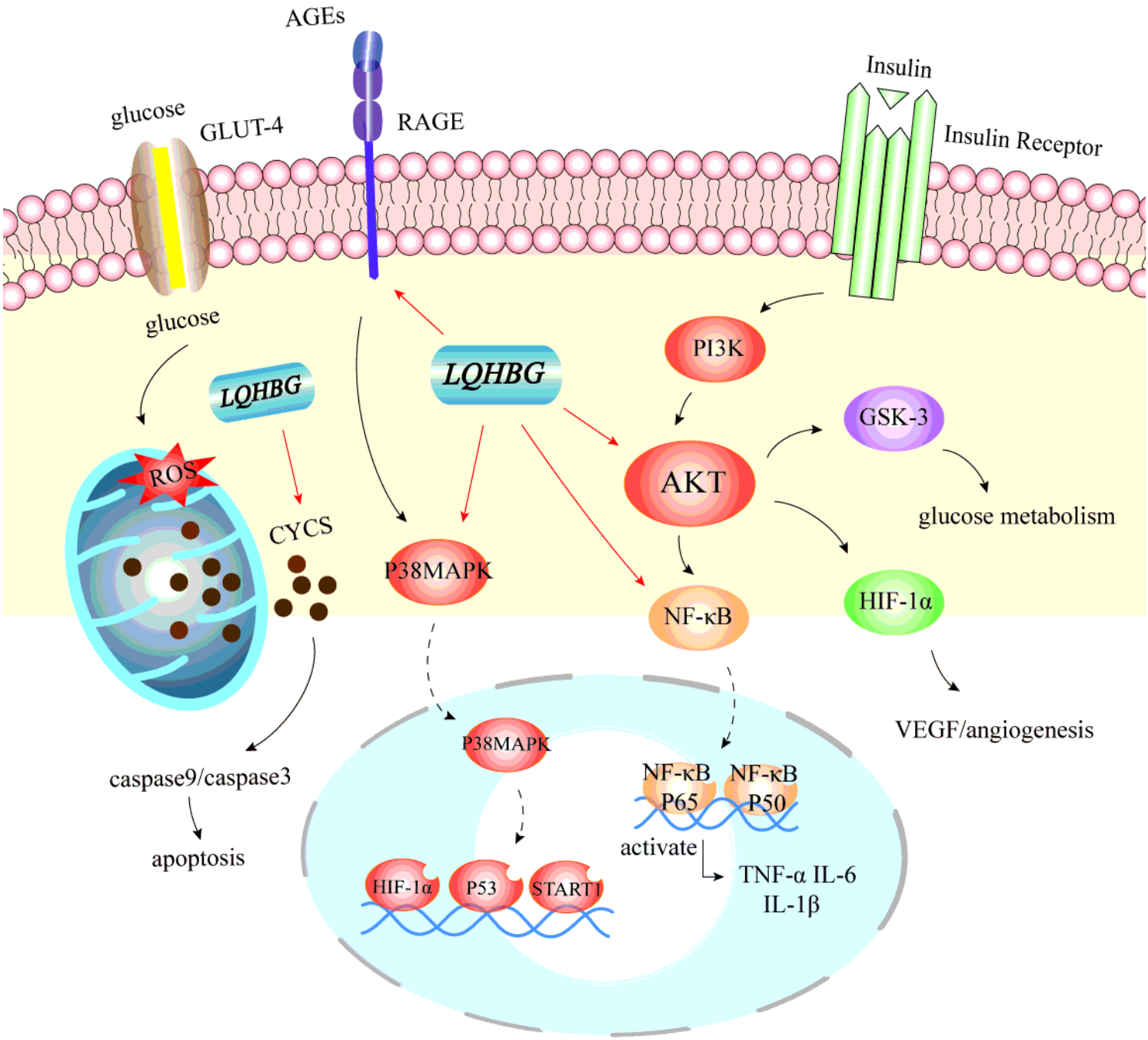

Figure 7

Potential mechanisms of LQHBG for treatment of DR

Supplementary Files

This is a list of supplementary files associated with this preprint. Click to download.

- Supplementaryfiles.xlsx
- Supplementaryfiles.docx
- Graphicabstract.tif